659. Comparative studies of computation tools for moving force identification

Qiong You[1], Zhiyu Shi[2], S. S. Law[3]
[1, 2] College of Aerospace Engineering, Nanjing University of Aeronautics and Astronautics, Yudao Street No. 29, Nanjing, Jiangsu, 210016, China
[3] Civil and Structure Engineering Department, the Hong Kong Polytechnic University, Hong Kong, China
E-mail: [1]*youqiong85@gmail.com*, [2]*zyshi@nuaa.edu.cn*

(Received 15 June 2011; accepted 5 September 2011)

Abstract. Existing techniques to identify moving forces based on traditional finite element method (TFEM) is subject to a large number of elements with detailed description of a structure, which makes modeling complicated. A new modeling method for a vehicle-bridge system called wavelet finite element method (WFEM) is presented in this paper. It makes use of a multi-scale analysis whereby detailed description can be achieved to overcome this problem. The shape function of WFEM is formed by a scale function in a wavelet space and by a transformation matrix to connect the wavelet space to the physical one. To evaluate the properties of WFEM, simulations of two moving forces on a simply supported and a continuous bridge are conducted with subsequent comparison with TFEM. To smooth the noise and large fluctuations on the boundaries of the identified results in the time history, the first-order Tikhonov regularizations combined with the dynamic programming technique are adapted and compared with the zeroth-order Tikhonov regularization. White noise is added to the simulated dynamic responses. Some parameter effects, such as vehicle bridge parameters, measurement parameters are also considered. Numerical results demonstrate the WFEM method and the first-order Tikhonov regularization method to be effective for moving force identification. The first-order Tikhonov regularization has the property of smoothing noise and avoiding large fluctuations on the boundaries. Meanwhile, the parameters analyzed affect the identified results to some extent.

Keywords: wavelet, multi-resolution, scale function, transformation matrix, dynamic programming technique, first-order Tikhonov regularization.

1. INTRODUCTION

Most existing moving force identification methods are based on traditional finite element method (TFEM) for its ripe theory, simply understood nature and developed software support. Some new finite element methods were proposed recently including generalized conforming element method [1], spline finite element method [2], meshless finite element method [3] and others [4]. During the last few decades, a new finite element method was developed - wavelet finite element method (WFEM). It aims at solving problems with singularity like greatly changed gradient in numerical calculation and cracks which can not be overcome based on TFEM. The WFEM not only can well deal with complicated boundaries the same as TFEM, but also provide a refined algorithm with high precision according to its unique multi-scale and multi-resolution features. The WFEM was formally brought forward by KO [5] as early as 1995, and it was applied for solving simple mathematical equations. Spline wavelet finite element was subsequently constructed by CHEN [6-7] to analyze dynamic problems in truss and membrane structures. B-spline wavelet on the interval (BSWI) was developed by HE et al [8-11], vibration analysis [12-13] and simply damage diagnosis [14-15] on different structure models were done based on it.

Generally speaking, it is still in the beginning stage of WFEM. Most of the studies focused on the benefit of the positive problems such as developing a model with accuracy based on WFEM, and analyzing of the dynamic behavior of vibration to ensure the correctness of the model.

However, it is without meaning for an engineering problem if such a theoretical model can not solve negative problems or can not be superior to the model based on TFEM.

Dynamic moving force is an important aspect of the problem of bridge-vehicle system, as not only for the bridge design and the management of highway pavement, but also for their monitoring and retrofitting in the transportation engineering. Calculation or direct measurement of the interaction moving force between vehicle and the bridge is usually subject to bias and is expensive, e.g. the Weigh-in Motion systems [16]. In the recent years, great effort has been made for moving force identification of bridge-vehicle system [17-30], and acceptable accuracy was yielded to meet this need. The identification problem was resolved by time domain method (TDM) [17-18], (time-frequency domain method) TFDM [19] and others [20-21]. The theoretical basis of the methods was categorized into two types, i.e. the exact solution method (ESM) [22] and TFEM [18, 23-24]. The bridge was generally modeled as a Euler-Bernoulli beam [25] or Timoshenko beam [26] or an orthotropic rectangular plate [23, 24]. The section could be uniformed [25] or non-uniformed [26]. The span could be single [27] or multi [25-26]. The bearings were stiff [27] or elastic [28]. There were also many studies on comparison of these methods and model conditions [29-30], in this paper, comparison are not all the same as those ones.

Such inverse dynamics problem, concerned with the estimation of unknown applied moving forces based on measured data, falls into a class of problems called ill-conditioned because the solution is extremely sensitive to the noise that was always present in the measurements. One successful approach to these problems was the zeroth-order Tikhonov regularization, which was also called the least squares error method [31-32] and was applied to provide bounds to the identified forces in the time domain. But for measurements polluted with high level noise, the identified results were coarse [26] and with large fluctuations. The first-order Tikhonov regularization was proposed by TRUJILLO [33-34] which could make sure the continuity of identified parameters and smooth the data. Here it will be employed to optimize the identified moving forces compared with zeroth-order regularization technique.

In this paper the WFEM is applied for modeling of vehicle-bridge system and subsequently compared with TFEM. The validations of the property of the proposed modeling method are demonstrated by identifying the moving forces on two kinds of vehicle-bridge system models: a simply supported beam model and a continuous bridge model, polluted with noise of different levels, employing different dynamic measurement data, arranging different locations and number of sensors. There are so many methods for moving force identification [17-21], here the dynamic programming technique [35] and Tikhonov regularization method are adapted for the moving force identification in the work. Numerical results demonstrate that the WFEM yields similar or more accurate results with respect to the TFEM under the same condition, and the scales of WFEM can be conveniently changed and to achieve different identification precisions, meanwhile the first-order Tikhonov regularization has a great benefit for avoiding large fluctuations and smoothing noise distinctly on the continuous bridge model polluted with high level noise.

2. THE VEHICLE-BRIDGE SYSTEM

In practice the bridge-vehicle system is a very complicated system. Normally, the bridge decks are modeled as beams or orthotropic rectangular plates. The use of simplified models is more effective to establish a clear connection between the moving force and the bridge response than a complex model. Thus Euler-Bernoulli beams, in which the effects of shear deformation and rotary inertia are not taken into account are employed in this paper. The vehicles are simulated as a two-axle moving forces with a fixed distance for simple analysis of vehicle-bridge interaction.

3. WFEM MODEL

3.1 Derivation of Transformation Matrix

In TFEM, piecewise polynomial and spline function are used as the interpolation function. In WFEM, (B-spline wavelet on the interval) BSWI is selected for constructing wavelet elements as an interpolation function in the wavelet space for its definite analytic expression in sections compared with other kinds of wavelet function.

In order to satisfy the continuity and compatibility of displacements in the boundaries, and to conveniently introduce boundary conditions, it is necessary to transform the system stiffness and mass matrix from wavelet space to physical space, correspondingly transform the DOFs of each element from wavelet parameters to physical unknown field function. So, it's the basement of WFEM to bring in a transform matrix, which is a key point for elemental construction.

An arbitrary unknown field function is expressed as follows in wavelet space:

$$w(\xi)=\sum_{k=-m+1}^{2^r-1} a^r{}_{m,k}\phi^r{}_{m,k}(\xi)=\Phi\{a^e\} \tag{1}$$

in which, $a^e=\left[a^r{}_{m,-m+1}\quad a^r{}_{m,-m+2}\cdots a^r{}_{m,2^r-1}\right]^T$ indicates a column vector of wavelet interpolating parameters; $\Phi=\left[\phi^r{}_{m,-m+1}(\xi)\quad \phi^r{}_{m,-m+2}(\xi)\cdots\phi^r{}_{m,2^r-1}(\xi)\right]$ indicates a row vector of scale function with m order and r scale.

On account of the continuity and compatibility in the boundaries of the element based on a Bernoulli-Euler beam model, two DOFs including the unknown field function w and the derivation of w should be considered, while only lateral displacements of the nodes within the element were taken into account. So there are $n+3$ DOFs in one wavelet finite element, and the physical DOFs could be defined by:

$$\{w^e\}=\left[w(\xi_1)\quad \frac{1}{l_e}\frac{dw(\xi)}{d\xi}|\,\xi=\xi_1\quad w(\xi_2)\quad\cdots\quad w(\xi_n)\quad w(\xi_{n+1})\quad \frac{1}{l_e}\frac{dw(\xi)}{d\xi}|\,\xi=\xi_{n+1}\right]^T \tag{2}$$

where e denotes an element. $\frac{1}{l_e}\frac{dw(\xi)}{d\xi}|\,\xi=\xi_1$ and $\frac{1}{l_e}\frac{dw(\xi)}{d\xi}|\,\xi=\xi_{n+1}$ denote the DOFs of rotation angles on the boundaries.

Substituting Eq. (1) with $w(\xi_i)$ on different nodes into Eq. (2), a formulation then is given by:

$$\{w^e\}=[R^e]\{a^e\} \tag{3}$$

in which matrix $[R^e]$ is defined by:

$$[R^e]=\left[\Phi^T(\xi_1)\quad \frac{1}{l_e}\frac{d\Phi^T(\xi)}{d\xi}|\,\xi=\xi_1\quad \Phi^T(\xi_2)\quad\cdots\quad \Phi^T(\xi_n)\quad \Phi^T(\xi_{n+1})\quad \frac{1}{l_e}\frac{d\Phi^T(\xi)}{d\xi}|\,\xi=\xi_{n+1}\right]^T \tag{4}$$

Substituting Eq. (3) into Eq. (1), an expression then should be given as:

$$w(\xi)=\Phi([R^e])^{-1}\{w^e\}=N^e\{w^e\} \tag{5}$$

in which,

$$N^e=\Phi([R^e])^{-1} \tag{6}$$

N^e is the shape function of the wavelet finite element.

Rewrite Eq. (6) with:

$$[T^e]=([R^e])^{-1} \tag{7}$$

the relationship between wavelet space and physical space is obviously obtained by:

$$N^e = \Phi\left[T^e\right] \tag{8}$$

in which, transform matrix $\left[T^e\right]$ connects the scale function Φ in wavelet space with the shape function N^e of wavelet finite element in physical space.

3.2 Construction of a beam element based on WFEM using BSWI

For a Euler-Bernoulli beam, the rotational angle is represented by a first-order derivation of the lateral displacement according to the theory of classical bending beams. The potential energy functional of such a beam element is given by:

$$\Pi(w) = \int_a^b \frac{EI}{2}\left(-\frac{d^2w}{dx^2}\right)^2 dx - \int_a^b q(x)w dx - \sum_j P_j w(x_j) + \sum_k M_k\left(\frac{dw}{dx}\right)_k \tag{9}$$

where EI is the bending stiffness, $w(x)$ is the mid-plane deflection function of the beam element. $q(x)$ denotes the distributed load, P_j denotes the concentrated load, M_k denotes the concentrated bending moment, x_j is the position coordinate of action point in the elemental solving domain, $\left(\frac{dw}{dx}\right)_k$ means the value of rotation angle at the action point of the concentrated bending moment.

Substituting Eq. (9) into Eq. (5) after the solving domain Ω_i has been mapped into standard solving domain Ω_s. Assuming $\partial\Pi = 0$ according to the variational principle, the solving equation in one element can be expressed as:

$$\left[K^e\right]\left\{w^e\right\} = \left\{P^e{}_w\right\} + \left\{P^e{}_{w_j}\right\} + \left\{P^e{}_{M_k}\right\} \tag{10}$$

in which, the stiffness matrix of each element is defined as:

$$\left[K^e\right] = \frac{EI}{l_e^3}\int_0^1 \left(\left[T^e\right]\right)^T \frac{d^2\Phi^T}{d\xi^2}\frac{d^2\Phi}{d\xi^2}\left[T^e\right] d\xi \tag{11}$$

the force vector under concentrated load is expressed as:

$$\left\{P^e{}_{w_j}\right\} = \sum_j P_j \left(\left[T^e\right]\right)^T \Phi^T\left(\xi_j\right) \tag{12}$$

The deduction of elemental mass matrix in the wavelet domain is similar to that for the stiffness matrix based on the potential energy representation of the system giving:

$$\left[M^e\right] = l_e \rho A \int_0^1 \left(\left[T^e\right]\right)^T \Phi^T \Phi \left[T^e\right] d\xi \tag{13}$$

in which, ρ means the density of material , A means the square of cross-section of the beam model.

Since Eq. (11) and Eq. (15) are obtained, which give the expression of each physical parameter based on wavelet space using BSWI in a beam element, the consequent processing was the same as TFEM, considering that:

$$[M] = \sum_{i=1}^{s}\left[M^e\right], \quad [K] = \sum_{i=1}^{s}\left[K^e\right], \quad [C] = \alpha[M] + \beta[K],$$

$$\{P\} = \sum_{i=1}^{s}\left(\left\{P^e{}_w\right\} + \left\{P^e{}_{w_j}\right\} + \left\{P^e{}_{M_k}\right\}\right) = [Y]\{f\}$$

where s represents the total number of elements, α, β are parameters decided by the first several natural frequencies of the beam model and $[C]$ indicates a Rayleigh damping matrix.

$\{f\}$ denotes the vector of actual moving forces and $[Y]$ signifies a time-varying location matrix relating to the moving forces. $[M]$, $[C]$ and $[K]$ represent global system mass, damping and stiffness matrices respectively.

4. METHOD FOR MOVING FORCE IDENTIFICATION

4.1 State-space equations:

Using the state-space formulation, the equilibrium equation of motion was converted into discrete forms using standard exponential representation as follows [35]:

$$\{X\}_{j+1} = [FF]\{X\}_j + [G]_{j+1}\{f\}_j \tag{14}$$

where $[FF] = e^{[K^*]\Delta t}{}_{2nn\times 2nn}$, $[K^*] = \begin{bmatrix} 0 & [I] \\ -[M]^{-1}[K] & -[M]^{-1}[C] \end{bmatrix}_{2nn\times 2nn}$,

and $[G] = [\overline{G}]_{2nn\times 2nn}\begin{bmatrix} 0 \\ [M]^{-1}[Y] \end{bmatrix}_{2nn\times nf}$, $[\overline{G}] = [K^*]^{-1}{}_{2nn\times 2nn}([FF]-[I])_{2nn\times 2nn}$

in which $[\overline{G}]$ represents the dynamic characters of the system here. j means the jth time step of computation, nn is the DOFs of the total system and nf is the number of the acting moving forces.

In the general formulation of the inverse problem, it was possible to replace the regularization term with the derivative of unknown forces instead of the forces themselves [33]. Eq. (14) then is rewritten as follows for the first-order system:

$$\{\overline{X}\}_{j+1} = [J]_{j+1}\{\overline{X}\}_j + [W]\{\dot{f}\}_j \tag{15}$$

in which, $\{\overline{X}\}_{j+1} = \begin{Bmatrix} \{X\}_{j+1} \\ \{f\}_{j+1} \end{Bmatrix}$ is a vector of state variables with dimension $(2nn+nf)\times 1$, $\{\dot{f}\}$ is the first-order derivative of the unknown forces with dimension $(nf)\times 1$ with:

$$[J] = \begin{bmatrix} [FF] & [G] \\ 0 & [I] \end{bmatrix}_{(2nn+nf)\times(2nn+nf)}, \quad [W] = \begin{bmatrix} 0 \\ I \end{bmatrix}_{(2nn+nf)\times nf}$$

The moving forces would be identified from Eq. (15) if the system matrices are known.

4.2 Problems and identified methods

The aim of this paper is to find a value of the forcing term $\{f\}$ to best match the measured forces. In practice, it is not possible to measure all of the displacements, velocities or the accelerations, only certain combinations of the variables $\{\overline{X}\}$ are measured. The simultaneous measured vector could be defined by:

$$\{Z\}_{2ns\times 1} = [Q]_{2ns\times 2nn}\{\overline{X}\}_{2nn\times 1} \tag{16}$$

where the number of simultaneous measured points ns is usually much less than the number of DOFs of the system. In this condition, the problem of this paper is solved by set up of a non-linear least-squares minimization procedure referred to as the zeroth-order Tikhonov regularization.

Therefore, the first-order Tikhonov regularization can be deduced upon the first-order system as follows:

$$E(\overline{X}_m, \dot{f}_m) = \sum_{m=1}^{ns}\left[\left(\{Z\}_m - [Q]\{\overline{X}\}_m\right),[A]\left([Z]_m - [Q]\{\overline{X}\}_m\right) + \left(\{\dot{f}\}_m,[B]\{\dot{f}\}_m\right)\right] \tag{17}$$

In which (x, y) denotes the inner product of two vectors x and y. $[A]$ is usually a $ns \times ns$ identity matrix, and $[B]$ is a $nf \times nf$ diagonal matrix containing the optimal regularization parameter λ. $[A]$, $[B]$ are weighting matrix and $[B]$ has the effect of smoothing the identified forces.

In order to obtain the identified moving forces by minimizing the value of error E in Eq. (17), the dynamic programming technique and Bellman's Principle of Optimality [36] are applied to find out the minimum value optimized by an optimal regularization parameter λ. A derivative formula using Bellman's Principle of Optimality about Eq. (17) is given by:

$$g_{j-1}(\overline{X}) = \min_{\dot{f}_{j-1}}\left[\left(\{Z\}_{j-1} - [Q]\{\overline{X}\}_{j-1}\right), [A]\left(\{Z\}_{j-1} - [Q]\{\overline{X}\}_{j-1}\right) + \left(\{\dot{f}\}_{j-1}, [B]\{\dot{f}\}_{j-1}\right)\right] + g_j\left([J]\{\overline{X}\}_{j-1} + [W]\{\dot{f}\}_{j-1}\right) \tag{18}$$

$\{\dot{f}\}_j$ and g_j present the optimal derivative of the force and optimal cost respectively. The optimal cost will be obtained by an appropriate $\{\dot{f}\}_j$, which is determined by the optimal regularization parameter λ. Eq. (18) can be expressed by:

$$g_j(\overline{X}) = q_j + \left(\{\overline{X}\}, \{S\}_j\right) + \left(\{\overline{X}\}, [R]_j \{\overline{X}\}\right) \tag{19}$$

where the variables are defined by:

$$q_j = \left(\{Z\}_j, [A]\{Z\}_j\right), \{S\}_j = -2[Q]_j^T [A]\{Z\}_j, [R]_j = [Q]_j^T [A][Q]_j \tag{20}$$

The iterative solution starts at the end of the process, where $j = N$. Then the subsequent variables in the $j-1$th step are expressed by variables in the j th step. Once all the variables are determined in the backward sweep, the optimal derivative force will be deduced and expressed by these variables in a forward sweep as:

$$\{\dot{f}\}_{j-1} = -\left([B] + [W]^T [R]_j [W]\right)^{-1} [W]^T \left([R]_j [J]_j \{\overline{X}\}_{j-1} + \frac{\{S\}_j}{2}\right) \tag{21}$$

Furthermore, the moving forces $\{f\}_j$ will then be obtained from Eq. (15).

As we all known L-curve was an efficient and accurate method seeking for the location of the optimal regularization parameter [31]. Thus, the following norms will be plotted to produce the L-curves for the first-order Tikhonov regularization:

$$E^2{}_{norm} = \sum_{j=1}^{N}\left(\{Z\}_j - [Q]\{\overline{X}\}_j, [A]\left(\{Z\}_j - [Q]\{\overline{X}\}_j\right)\right), \quad F^2{}_{norm} = \sum_{j=1}^{N}\left(\{\dot{f}\}_j, \{\dot{f}\}_j\right) \tag{22}$$

It is clear that when the system is at rest, the initial optimal condition is zeros for the upper part of the state vector $\{\overline{X}\}_1$ and the initial value for the unknown forces in the lower part of the state vector $\{\overline{X}\}_1$ can be found by averaging the value of the identified moving forces without the beginning and ending parts in a guess trial of the estimation process. However if the bridge wasn't at rest at the beginning, the initial optimal condition would be given by [34]:

$$\begin{Bmatrix}\{X\}_1 \\ \{f\}_1\end{Bmatrix} = -[R]_1^{-1}\{S\}_1/2 \tag{23}$$

from Eq. (19).

5. SIMULATION CASES AND ANALYSIS

5.1 Identification of moving forces from a simply supported beam

In order to check the correctness of the above-mentioned modeling method, two time-varying moving forces are simulated as follows:

$$P_1(t) = 20000(1 + 0.1\sin(10\pi t) + 0.05\sin(40\pi t))$$

$$P_2(t) = 20000(1 - 0.1\sin(10\pi t) + 0.05\sin(40\pi t))$$

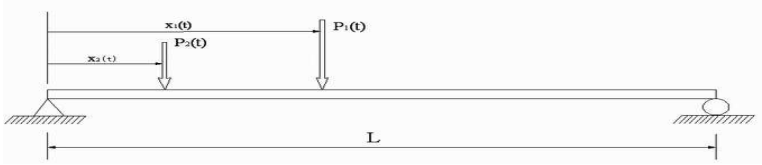

Fig. 1. Vehicle-Bridge model under moving forces

The two forces represent a vehicle with a static gross weight of 40000N, and with a fixed axle spacing of 4-meters, moving with a constant velocity of 40 m/s over the bridge.

A 40-meters simply supported Bernoulli-Euler beam with a bending stiffness of *EI* $=1.2749\times10^{11}$ Nm^2 is modeled as the bridge, with a length density of 1.2×10^4 kg/m. The first three frequencies of this beam are f_1 =3.2 Hz, f_2 =12.8 Hz and f_3 =28.8 Hz respectively. The sampling frequency should be selected twice higher the first five vibration modes and limited by the computation capacity. Therefore, the optimum value of 400 Hz is selected as the sampling frequency during the calculation. The first three damping ratios were ζ_1=0.02, ζ_2=0.02 and ζ_3=0.04 respectively. The model system has a Rayleigh damping and the corresponding two parameters are α =0.64344 and $\beta = 3.9779\times10^{-4}$ respectively.

The bridge model is divided into 8 TFEM elements which usually is enough for the required precision of identified moving forces. To figure out the advantage of the WFEM compared with the TFEM, only 1 WFEM element is chosen for identification. Scales 3 and 4 are employed to validate the multi-scale property of WFEM.

According to the simulated forces, the simulated dynamic responses at different locations of the beam will be calculated using Newmark method respectively, which are forward problems. White noise is added to the calculated responses to simulate the polluted measurements. To evaluate the modeling method and the identification accuracy, the relative percentage error (RPE) between the true and identified forces are calculated for different models, identification methods or different location and number of sensors as follows:

$$\text{Error} = \frac{\sum\left|f_{true} - f_{identified}\right|}{\sum\left|f_{true}\right|} \times 100\% \tag{24}$$

In Eq. (24), the true force is the simulated time-varying moving forces and the identified force will be obtained by solving inverse problem as stated in Eq. (14) or Eq. (15) depending on different regularization methods.

5.1.1 First-order Tikhonov regularization procedure compared with zeroth-order one

The displacements and velocities are simulated by Newmark method as the applied dynamic responses, and seven sensors are equally spaced along the beam.

With zeroth-order and first-order Tikhonov regularization methods, figures 2 and 3 show the identified moving forces based on TFEM and WFEM models with 10 percent noise level, Tables 1 and 2 give the RPE results between the true and the identified forces applying different noise levels, different modeling methods and different scales with WFEM.

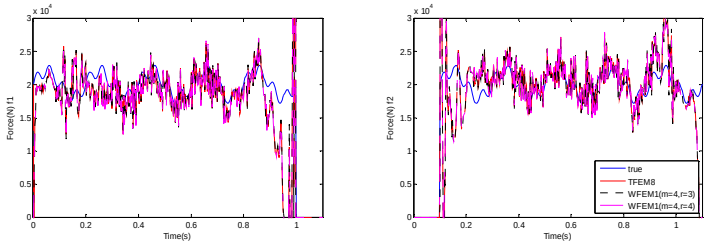

Fig. 2. Identification with 10% noise with zeroth-order Tikhonov regularization

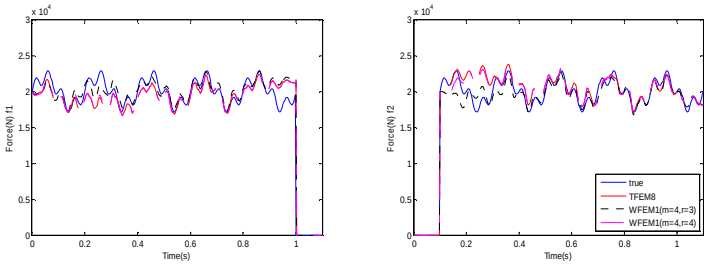

Fig. 3. Identification with 10% noise with first-order Tikhonov regularization

Table 1. RPE values in two forces identification (%) with zeroth-order Tikhonov regularization

		Errors (%)		
	Noise level (%)	0	5	10
f_1	TFEM 8 elements	9.92	16.46	30.53
	WFEM (*m=4,r=3*) 1 element	9.94	16.98	31.59
	WFEM (*m=4,r=4*) 1 element	10.6	15.83	28.97
f_2	TFEM 8 elements	10.11	14.55	27.62
	WFEM (*m=4,r=3*) 1 element	10.06	14.70	27.73
	WFEM (m=4,r=4*) 1 element*	10.48	14.42	26.82

Table 2. RPE values in two forces identification (%) between two regularization methods with WFEM

WFEM (*m=4, j=3*)		*Error (%)*		
	Noise level (%)	0	5	10
f_1	Tikhonov regularization	9.47	15.09	28.57
	First-order regularization	7.96	8.10	8.47
f_2	Tikhonov regularization	10.55	14.44	26.82
	First-order regularization	6.38	6.39	6.68

Table 3. Computational time required for the zeroth-order Tikhonov regularization solution

	Computational time (second)		
Noise level (%)	0	5	10
TFEM 8 elements	4.4	4.7	4.8
WFEM (*m=4,r=3*) 1 element	3.5	4.5	4.4
WFEM (*m=4,r=4*) 1 element	4.8	4.8	4.8

Table 4. Computational time required for the first-order Tikhonov regularization solution

	Computational time (second)		
Noise level (%)	0	5	10
TFEM 8 elements	7.7	7.6	7.6
WFEM (*m=4,r=3*) 1 element	5.1	5.0	5.1
WFEM (*m=4,r=4*) 1 element	7.9	8.1	8.0

Tables 3 and 4 note the computational time required from different modeling methods and noise levels. From the analysis of the above mentioned figures and tables, the following comments are given:

(1) From Figs. 2 and 3, the identified black and pink lines are close to the true value ones under both zeroth and first-order Tikhonov regularization methods. It indicates that it is feasible for WFEM model to identify moving force using displacements and velocities as simulated dynamic responses.

(2) The errors between the identified and true forces decrease with the increase of the scales of WFEM in Table 1, when the noise is polluted into the simulated dynamic responses. This indicates that it's capable for the property of multi-scale of WFEM to affect the precision of force identification.

(3) The RPE values are similar under WFEM 1 element models compared with TFEM 8 elements model. It means the WFEM takes the advantage of much fewer elements compared to TFEM for a similar identification precision.

(4) When the scales are adopted from 3 to 4, more computation effort is needed for moving force identification. Comparing the computation time between TFEM and WFEM, it reveals that similar or less computation efforts are needed of WFEM for similar identification accuracy.

(5) Figs. 2 and 3 provide the identified moving forces using the simulated dynamic responses polluted with a high level noise of 10%. The results not only illustrate the first-order Tikhonov regularization has a strong capability of avoiding the large fluctuations on the boundaries and smoothing out the high frequency components during the identified force time histories, but also mean that the first-order Tikhonov regularization technique is noise non-sensitive while the zeroth-order one is noise sensitive.

5.1.2 Effects of parameters on identification accuracy

Many parameters influence the moving force identification problem and it is necessary to study their effects on the identification methods. Some effects of the main parameters, such as bridge-vehicle parameters (vehicle speed) and measurement parameters (frequency, measurement number and stations), are reported here.

For vehicle speed:

Scale 3 and 4 of WFEM are chosen for modeling with 1 element and the dynamic responses of displacements and velocities with and without noise are used for moving force identification respectively. Fig. 4 and Fig. 5 reveal that the identification RPEs vary with the vehicle speeds. Some recommendations during the consideration of speed area are:

(1) When the dynamic responses are without noise, the RPE values of both the two axle loads are varying slowly. When the vehicle speed increases, the RPE of the identified front axle (light axle) load rises while the RPE of the rear axle (heavy axle) load drops.

(2) When the dynamic responses are with noise, the best RPEs are obtained under the vehicle speed with 20 m/s on such models. So for the general engineering problem considering noise, the best identified results of moving forces will be obtained if the vehicle speed is about 72 km/h for the simulated vehicle used in this paper. That means the best method for achieving the two-axle vehicle loads which are most close to the real ones is to monitor the corresponding vehicles moving on the highway bridges.

For sampling frequency:

Fig. 6 illustrates the effect of sampling frequency on the WFEM and TFEM models with the zeorth order Tikhonov regularization using dynamic responses polluted with 5% noise. The best sampling frequency for such a model is around 400 Hz. The identified RPEs are divergent when the sampling frequency is above 480 Hz, while the RPEs of identified moving force are too large and unstable when the sampling frequency is too small. Meanwhile, the RPEs on WFEM model are more sensitive to sampling frequency than the ones on TFEM model.

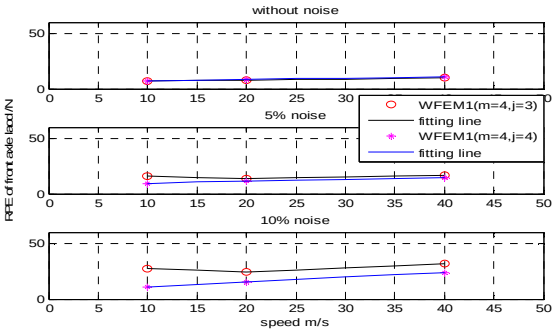

Fig. 4. The identification RPEs of the front axle load

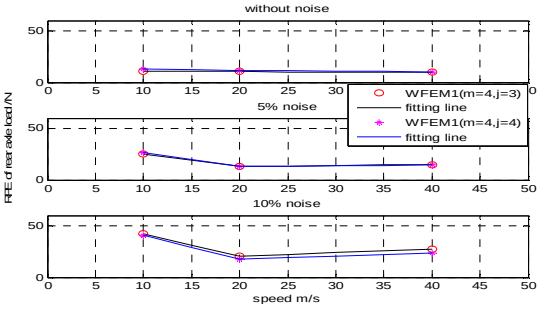

Fig. 5. The identification RPEs of the rear axle load

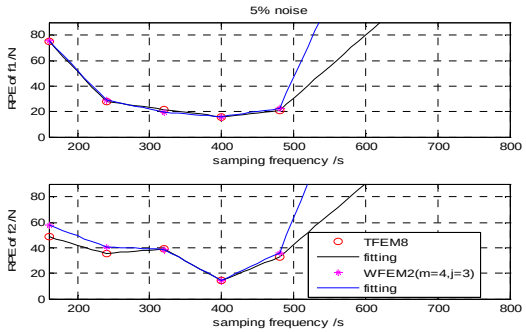

Fig. 6. The identification RPEs with zeroth-order Tikhonov regularization

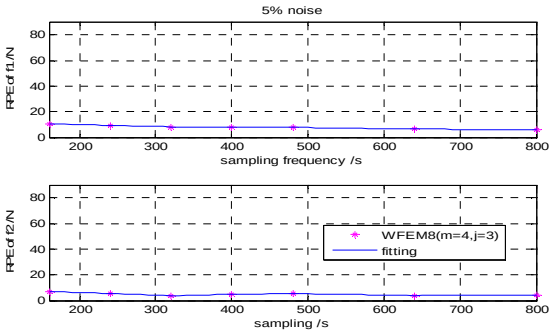

Fig. 7. The identification RPEs with first-order Tikhonov regularization

Fig. 7 presents the effect of sampling frequency on the WFEM model with the first-order Tikhonov regularization using dynamic responses polluted with 5% noise. The RPEs vary bit by bit along the increasing of sampling frequency. Compared with Fig 6, it is obvious that the identification results are nearly non-sensitive to sampling frequency based on WFEM model with the first-order Tikhonov regularization.

For sensor number and stations:

Scale 4 of WFEM is chosen for modeling with 1 element to compare with TFEM 8 elements. The simulated accelerations are applied as the dynamic measurements with polluted noise components instead of the displacements and the velocities, which are much more close to practical condition. The analysis on force identification results is studied when the number of sensors changed from three to seven, or only the location of sensors is changed.

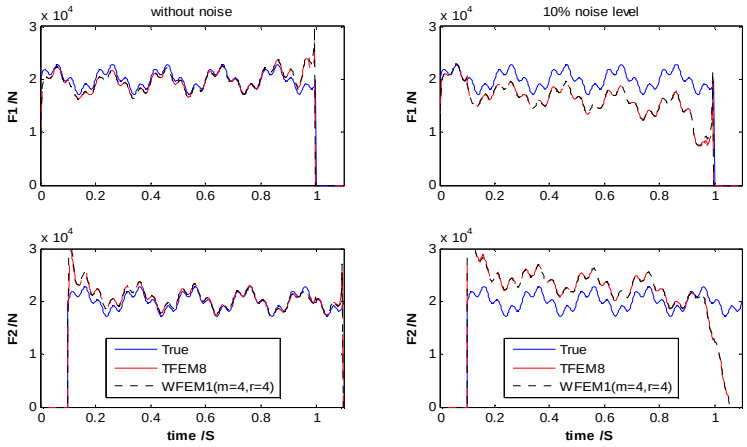

Fig. 8. The identification results based on TFEM and WFEM models with different noise levels

Table 5. RPE values with different number and location of sensors using acceleration responses

location	RPE (%)											
	TFEM 8 elements						WFEM ($m=4$, $r=4$) 1 element					
	0%		5%		10%		0%		5%		10%	
	f_1	f_2	f_1	f_2	f_1	f_2	f_1	f_2	f_1	f_2	f_1	f_2
1/8, 1/2, 7/8	28.61	43.7	29.3	45.38	30.06	46.94	*	*	*	*	*	*
3/8, 1/2, 5/8	28.21	35.41	28.48	36.82	28.79	37.67	*	*	*	*	*	*
1/4, 1/2, 3/4	23.41	27.92	24.25	31.19	25.2	33.97	23.4	27.94	24.24	31.2	25.18	33.98
1/8, 3/8, 1/2, 5/8, 7/8	10.36	9.97	12.71	23.79	21.17	34.71	10.9	10.34	12.82	24.43	21.0	35.39
1/4, 3/8, 1/2, 5/8, 3/4	26.62	33.16	26.96	34.82	27.35	36.27	*	*	*	*	*	*
1/8, 1/4, 1/2, 3/4, 7/8	9.91	10.0	13.87	24.89	25.78	36.85	10.50	10.45	13.5	25.49	24.86	37.39
Each 1/8 location	9.92	10.11	13.12	25.04	23.27	37.06	10.55	10.48	13.08	25.62	22.84	37.52

Note: * denotes RPE values > 50%

Zeroth-order Tikhonov regularization is employed for solving the inverse problem. Fig. 8 shows the identification results of moving forces polluted with different noise levels under both WFEM and TFEM models with seven sensors. Table 5 lists the RPE values with different numbers and locations of sensors. From the results presented the following may be noted:

(1) In Fig. 8 the identified lines of moving forces are close to the lines of true one. This indicates that it is successful for the WFEM model to obtain the identification solution with the simulated acceleration measurements.

(2) The figure and the table show that the RPE values are similar under WFEM 1 element model compared with TFEM 8 elements model. It signifies that the WFEM takes the advantage of much fewer elements compared to TFEM for the similar identification accuracy, when the location of sensors was properly arranged.

(3) In Table 5 the identification errors of moving forces with different noise level decreases totally when the number of sensors increases from 3 to 7. When the number of sensors varies to 5, one of the force identification results are close to the ones using 7 sensors. Such results illustrate that the number of sensors affects the identification RPEs, however it can be cut down if the location of sensors is with a proper arrangement.

(4) There are RPE values in Table 5 expressed as * when WFEM model applied. That notes the identification results with WFEM are much more sensitive than TFEM to the location of sensors even if the same number of sensors is adopted.

5.2 Identification of moving forces from a continuous bridge beam

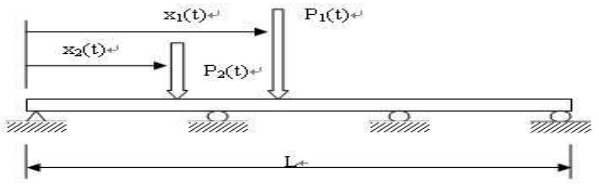

Fig. 9. The continuous vehicle-bridge model under moving forces

A continuous multi-span beam is used for WFEM modeling to further prove the studies done above. The moving forces are arranged along the axial direction of the beam at a speed of 32 m/s, and separated at a fix distance of 4 m. They are represented as follows consisting of a carrier force and two other components at higher frequencies:

$$P_1(t) = 15000(1 + 0.1\sin(10\pi t) + 0.05\sin(40\pi t))$$

$$P_2(t) = 25000\,(1 - 0.1\sin(10\pi t) + 0.05\sin(40\pi t))$$

The two forces simulate a vehicle with a static gross weight of 40 kN, similar to the above one, with the first and second static force being 15 and 25 kN, respectively, which will be much more close to the practical condition.

The bridge is modeled as a three span continuous beam over two internal supports, and simply supported over the two outer supports. The parameters of the beam are EI=1.2749×10^{11} Nm^2 and ρA=1.2×10^4 kg/m. The total length of the beam is 60 m and the length of each of the three spans is 20 m. The first three damping values were taken to be ζ =0.02 for all. The first three vibration modes are f_1=12.8 Hz, f_2=16.4 Hz and f_3=24.0 Hz, respectively. Reyleigh damping is assumed, and the corresponding damping coefficients are obtained from the damping and the natural frequencies.

The continuous beam model is equally divided into 12 TFEM elements and 3 WFEM elements, respectively. Scale 3 of WFEM is chosen to figure out the feasibility for moving force identification on the continuous bridge. The simulated acceleration measurements polluted with

noise are used for the inverse analysis taken account of the experimental instruments. Seven sensors are located on the continuous beam, with three of them equally spaced on the middle span and others arranged on the 1/4 and 3/4 positions of the side spans.

5.2.1 First-order Tikhonov regularization compared with zeroth-order one

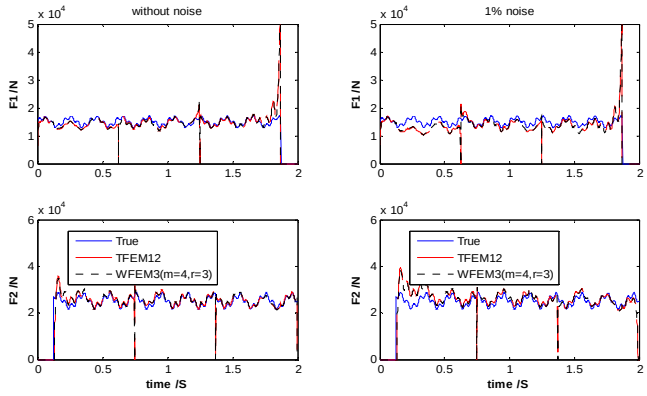

Fig. 10. The force identification results based on zeroth-order Tikhonov regularization with different noise levels

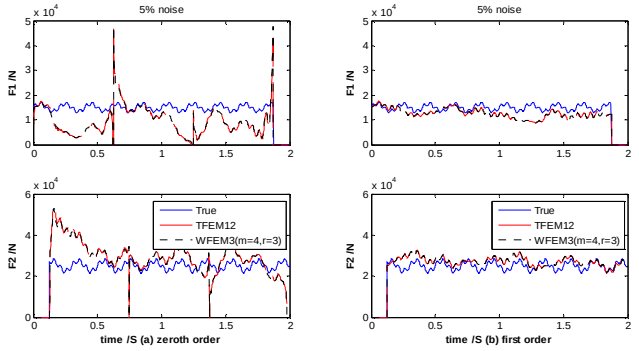

Fig. 11. Moving force identification with different Tikhonov regularizations

With zeroth-order Tikhonov regularization, the identified moving forces polluted with and without noise are shown as Fig. 10. With the first-order Tikhonov regularization, the identification result is presented in Fig. 11(b) compared with the zeroth-order one in Fig. 11 (a). The comparison RPE values between different regularization methods and noise levels with WFEM are noted in Table 6. Meanwhile, the computational effort required for each condition is also listed out in Table 7. From the results presented below, the following observations are made:
(1) In Fig. 10 the identified black and red lines are close to the true ones both with and without noise. This indicates that it is possible for WFEM to identify moving force using the simulated acceleration measurements on a continuous beam model.
(2) The identified lines of moving forces with WFEM 3 elements are close to the ones with TFEM 12 elements, especially at the parts of high frequency components, under both zeroth-order and first-order Tikhonov regularization methods. It indicates that the WFEM takes the advantage of much fewer elements compared to TFEM for a similar identification accuracy, as the same as on a simply supported beam.
(3) If the simulated dynamic responses are polluted with a 5% noise level, the identified moving forces with different Tikhonov regularization methods are as shown in Fig. 11. The results of

Fig. 11 (a) notes that the zeroth-order Tikhonov regularization could not avoid the effect of high level noise, the identification is ill-posed and almost loses true values, meanwhile, the comparison from Fig. 7 (b) illustrates that the first-order Tikhonov regularization has a strong capability to avoid the large fluctuations in the boundaries and the supporting points, and to smooth out the high frequency components including high level noise during the identified force time histories.

(4) As the noise level increases, the RPE values increase obviously in Table 6 with zeroth-order Tikhonov regularization. It denotes that the zeroth-order Tikhonov regularization is noise sensitive. The errors based on the first-order Tikhonov regularization solution increase relatively bit by bit with the increasing of noise levels. That remarks the first-order Tikhonov regularization comparatively is noise non-sensitive.

(5) Comparison of the computation time between TFEM and WFEM that the latter requires slightly more computational effort for similar identification accuracies. The first-order Tikhonov regularization takes more computation time compared to zeroth-order Tikhonov regularization as the cost for a higher precision. In short, the computational effort for all conditions is acceptable.

Table 6. RPE values in two forces identification (%) between two regularization methods under WFEM

WFEM (*m=4, j=3*)		*Error (%)*		
Noise level (%)		0	1	5
f_1	Tikhonov regularization	22.21	22.68	51.43
	First-order regularization	8.05	9.14	20.41
f_2	Tikhonov regularization	12.37	16.0	50.67
	First-order regularization	5.0	5.76	11.77

Table 7. Computation time required for different regularization methods and models

	Computational time (second)					
	Zeroth-order Tikhonov			First-order Tikhonov		
Noise level (%)	0	1	5	0	1	5
TFEM 12 elements	10.39	8.91	8.88	18.67	15.24	15.14
WFEM 3 elements	14.68	11.14	11.18	21.86	16.80	17.16

5.2.1 Effects of parameters on identification accuracy

Some effects of the main parameters, such as bridge-vehicle parameters (vehicle speed) and measurement parameters (frequency), are reported here.

For vehicle speed:

Based on the WFEM 3 elements and TFEM 12 elements model, Figs. 12 and 13 shows the identification RPEs change with vehicle speed using acceleration dynamic responses with and without noise. Some comments based on the results in the figures considering speed area:

(1) When the dynamic responses are without noise, the RPE values of both the two axle loads are varying quite slowly.

(2) When the dynamic responses are with noise, the acceptable identification RPEs should be above 20 m/s, the identification results are much better when the speed is raised.

For sampling frequency:

Figs. 14 and 15 illustrate the effect of sampling frequency on the WFEM and TFEM models with the zeroth and first-order Tikhonov regularization respectively using dynamic responses polluted with 5% noise.

The identification RPEs are unstable and out of the requirement when the sampling frequency is too low, and they are divergent when the sampling frequency is above 480 Hz with the zeroth-order Tikhonov regularization in Fig. 14. Comparatively, the identification RPEs are

stable and acceptable when the sampling frequency is above 250 Hz and the RPEs decrease with the increase of sampling frequency with the first-order Tikhonov regularization in Fig. 15.

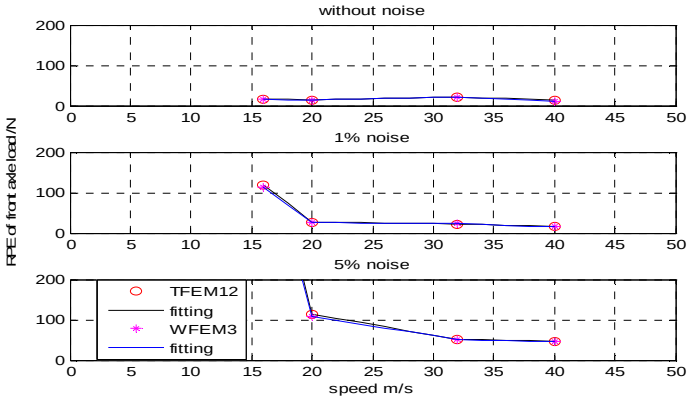

Fig. 12. The identification RPEs of the front axle load

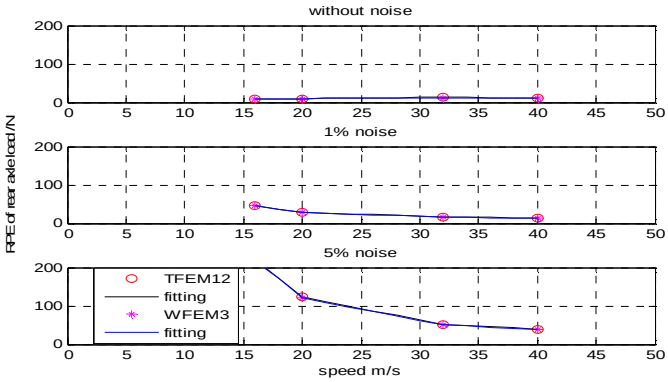

Fig. 13. The identification RPEs of the rear axle load

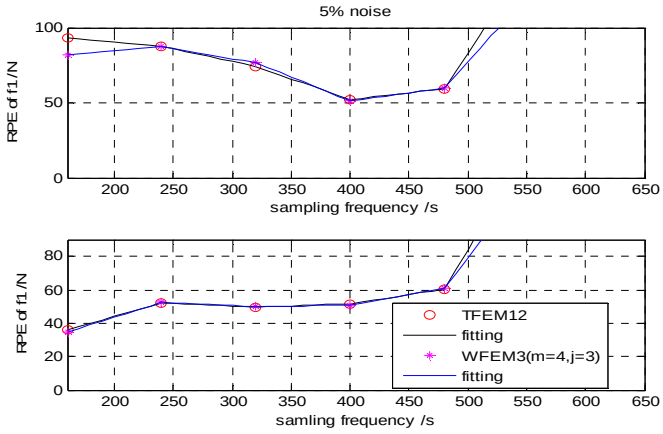

Fig. 14. The identification RPEs with zeroth-order Tikhonov regularization

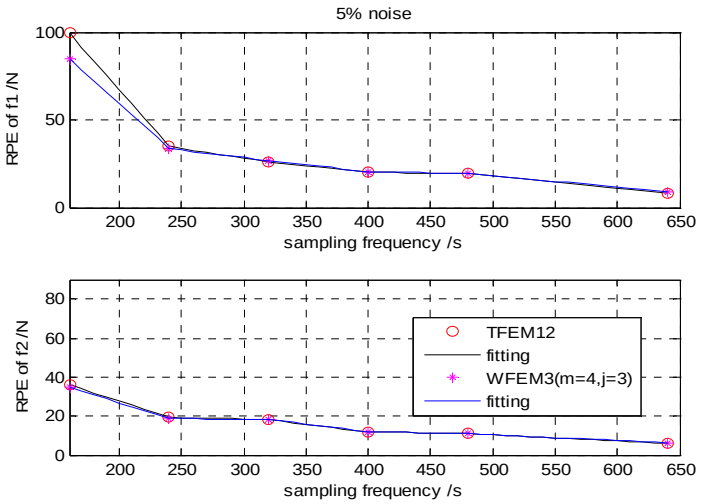

Fig. 15. The identification RPEs with the first-order Tikhonov regularization

6. CONCLUSIONS

The results presented above indicate that it is acceptable and successful to use WFEM model to accurately identify the moving vehicles on bridges, compared with TFEM. Comparative studies on modeling methods and moving force identification methods have been carried out. The effects of parameters, such as the scales of WFEM, the computational time, the sensor number and location, the sampling frequency, the vehicle speed and the influence of noise levels have been investigated respectively. The following conclusions are drawn. (1) The moving force identification with scale 4 yields a higher precision compared to scale 3, irrespective of noise levels and type of the dynamic responses used. (2) The identifications with WFEM and TFEM models both provide acceptable and close results neglecting the change of noise, while only few elements are needed for WFEM models. (3) Zeroth-order Tikhonov regularization is noise sensitive, when the model varies to more complicated and the noise level rises, the moving force identification results turn to unacceptable, as shown in Fig 11(a). The first-order Tikhonov regularization is comparatively noise non-sensitive. It has the capability to smooth out the high frequency components of the identified lines during the force time histories and to avoid the large fluctuations in the boundaries and supporting points at the same time. (4) The computation effect based on WFEM model and the first-order Tikhonov regularization has no direct connection with noise levels. (4) During the consideration of vehicle speed area, the RPE values change bit by bit along the increase of vehicle speed when the dynamic responses are without noise. But in practice the noise pollution is observed in the dynamic responses. For simply supported bridge, the best speed of two-axle vehicle for moving force identification is around 72 km/h. While for continuous bridge, the larger the speed the better. (5) The identification RPEs are obviously affected by the sampling frequency with zeroth-order Tikhonov regularization, and the RPEs on WFEM model are more sensitive to sampling frequency than the ones on TFEM model. Comparatively, the RPEs are acceptable and stable with the first-order Tikhonov regularization when the sampling frequency is above 250 Hz. That implies that the first-order Tikhonov regularization is non-sensitive to sampling frequency in some extent. (6) The WFEM is more sensitive than TFEM to the location of sensors when the same number of sensors is arranged (Table 5). The sensor number could be reduced to a comparatively low level if the location of sensors is properly selected.

ACKNOWLEDGEMENTS

The present project is supported by the National Natural Science Foundation of China through Grant No. 11172131, and by the Graduate Cultivation and Innovation Foundation of Jiangsu Province through Grant No. CX09B_071Z.

References

[1] Long Yu-qiu Generalized conforming element method [J]. China Civil Engineering Journal, 1987, 20(1): 1-14. (In Chinese).

[2] Cheung Y. K., Zhu D. S., Lu V. P. Nonlinear vibration of thin plates with initial stress by spline finite strip method [J]. Thin-Walled Structures, 1998, 32(4): 275-287.

[3] Song Kang-Zu, Lu M. W., Zhang X. Meshless method for solid mechanics [J]. Advance In Mechanics, 2000, 30(1): 55-65. (In Chinese).

[4] Gupta R. K., Babu G. J., Janardhan G. R. and et. al. Relatively simple finite element formulation for large amplitude free vibrations of uniform beams [J]. Finite Elements in Analysis and Design, 2009, 45(10): 599-611.

[5] Ko J., Kurdila A. J., Pilant M. S. A class of finite element methods based on orthonormal, compactly supported wavelets [J]. Computational Mechanics, 1995, 16(4): 235-244.

[6] Chen W. H., Wu C. W. Spline wavelets element method for frame structures vibration [J]. Computational Mechanics, 1995, 16(1): 11-21.

[7] Chen W. H., Wu C. W. Extension of spline wavelets element method to membrane vibration analysis [J]. Computational Mechanics, 1996, 18(1): 46-54.

[8] He Zheng-Jia, Chen Xue-Feng, Li Bin, et al. The theory and engineering application of wavelet finite element [M]. Beijing: Science Press, 2006. (In Chinese).

[9] Xiang J. W., Chen X. F., He Y. M., et al. The construction of plane elastomechanics and Mindlin plate elements of B-spline wavelet on the interval [J]. Finite Element in Analysis and Design, 2006, 42(14-15): 1269-1280.

[10] Xiang J. W., Chen X. F., Mo Q. Y., et al. Identification of crack in a rotor system based on wavelet finite element method [J]. Finite Elements in Analysis and Design, 2007, 43(14): 1068-1081.

[11] Xiang J. W., Chen D. D., Chen X. F., et al. A novel wavelet-based finite element method for the analysis of rotor-bearing systems [J]. Finite Element in Analysis and Design, 2009, 45(12): 908-916.

[12] Díaz A. L., Martín M. T., Vampa V. Daubechies wavelet beam and plate finite elements [J]. Finite Elements in Analysis and Design, 2009, 45(3): 200-209.

[13] Zhang X. W., Chen X. F., Wang X. Z., et al. Multivarialble finite elements based on B-spline wavelet on the interval for thin plate static and vibration analysis [J]. Finite Elements in Analysis and Design, 2010, 46(5): 416-427.

[14] Dong H. B., Chen X. F., Li B., et al. Rotor crack detection based on high-precision modal parameter identification method and wavelet finite element model [J]. Mechanical Systems and Signal Processing, 2009, 23(3): 869-883.

[15] Ye J. J., He Y. M., Chen X. F., et al. Pipe crack identification based on finite element method of second generation wavelets [J]. Mechanical Systems and Signal Processing, 2010, 24(2): 379-393.

[16] Moses F. Weigh-in-motion system using instrumented bridges [J]. Journal of Transport and Engineering, ASCE 1978, 105: 233-249.

[17] Law S. S., Chan T. H. T., Zeng Q. H. Moving Force Identification: A Time Domain Method [J]. Journal of Sound and Vibration, 1997, 201(1): 1-22.

[18] Zhu X. Q., Law S. S. Time Domain Identification of Moving Loads on Bridge Deck [J]. Journal of Vibration and Acoustics, ASME, 2003, 125(2): 187-198.

[19] Law S. S., Chan T. H. T., Zeng Q. H. Moving Force Identification: A Frequency and Time Domains Approach [J]. Journal of Dynamic Systems, Measurement and Control, ASME, 1999, 121(3): 394-401.

[20] O'Connor, Chan T. H. T. Dynamic wheel loads from bridge strains [J]. Journal of Structural Engineering, ASCE, 1988, 114: 1703-1723.

[21] Chan T. H. T., Law S. S., Yung T. H., et al. An interpretive method for moving force identification [J]. Journal of Sound Vibration, 1999, 219(3): 503-524.

[22] Zhu X. Q., Law S. S. Identification of Moving Loads on an Orthotropic Plate [J]. Journal of Vibration, ASME 2001, 123(2): 238-244.

[23] Lu Z. R., Law S. S. Identification of system parameters and input force from output only [J]. Mechanical Systems and Signal Processing, 2007, 21(5): 2099-2111.
[24] Zhu X. Q., Law S. S., Bu J. Q. A State Space Formulation for Moving Loads Identification [J]. Journal of Vibration and Acoustics, ASME, 2006, 128(4): 509-520.
[25] Chan T. H. T., Ashebo D. B. Theoretical study of moving force identification on continuous bridges [J]. Journal of Sound and Vibration, 2006, 295(3-5): 870-883.
[26] Zhu X. Q., Law S. S. Moving forces identification on a multi-span continuous bridge [J]. Journal of Sound and Vibration, 1999, 228(2): 377-396.
[27] Pinkaew T. Identification of vehicle axle loads from bridge response using updated static component technique [J]. Engineering Structures, 2006, 28: 1599-1608.
[28] Zhu X. Q., Law S. S. Moving load identification on multi-span continuous bridges with elastic bearings [J]. Mechanical Systems and Signal Processing, 2006, 20(7): 1759-1782.
[29] Chan T. H. T., Yu L., Law S. S. Comparative studies on moving force identification from bridge strains in laboratory [J]. Journal of Sound and Vibration, 2000, 235(1): 87-104.
[30] Yu L., Chan T. H. T. Recent research on identification of moving loads on bridges [J]. Journal of Sound and Vibration, 2007, 305(1-2): 3-21.
[31] Calvetti D., Morigi S., Reichel L., et al. Tikhonov regularization and the L-curve for large discrete ill-posed problems [J]. Journal of Computational and Applied Mathematics, 2000, 123(1-2): 423-446.
[32] Reichel L., Sgallari F., Ye Q. Tikhonov regularization based on generalized Krylov subspace methods [J]. Applied Numerical Mathematics, In Press.
[33] Busby H. R., Trujillo D. M. Optimal regularization of an inverse dynamics problem [J]. Computers and Structures, 1997, 63(2): 243-248.
[34] Gonzalez A., Rowley C., Obrien E. J. A general solution to the identification of moving forces on a bridge [J]. International Journal for Numerical Methods in Engineering, 2008, 75(3): 335-354.
[35] Law S. S., Fang Y. L. Moving force identification: optimal state estimation approach [J]. 2001, 239 (2): 233-254.
[36] Bellman R. Introduction to the Mathematical Theory of Control Processes [M]. New York: Academic Press. 1967.